

RESEARCH ARTICLE

 OPEN ACCESS

Received: 08.10.2021

Accepted: 17.02.2022

Published: 15.04.2022

Citation: Kalkhambkar G, Chindhi P, Khanai R (2022) Design and Finite Difference Time Domain Analysis of a Dual Band Slotted Microstrip Patch Antenna for Wireless IoT Applications. Indian Journal of Science and Technology 15(15): 668-676. <https://doi.org/10.17485/IJST/v15i15.1904>

* **Corresponding author.**geetakalkhambkar@gmail.com**Funding:** None**Competing Interests:** None

Copyright: © 2022 Kalkhambkar et al. This is an open access article distributed under the terms of the [Creative Commons Attribution License](https://creativecommons.org/licenses/by/4.0/), which permits unrestricted use, distribution, and reproduction in any medium, provided the original author and source are credited.

Published By Indian Society for Education and Environment ([iSee](https://www.indst.org/))

ISSN

Print: 0974-6846

Electronic: 0974-5645

Design and Finite Difference Time Domain Analysis of a Dual Band Slotted Microstrip Patch Antenna for Wireless IoT Applications

Geeta Kalkhambkar^{1*}, Pradeep Chindhi¹, Rajashri Khanai²

¹ Research Scholar, Department of Electronics and Communication, KLE Dr. MSSCET Belagavi, India

² Professor, Department of Electronics and Communication, KLE Dr. MSSCET, Belagavi, India

Abstract

Objectives: To investigate the effect of comb-like slot dimensions on the dual-band microstrip antenna performance parameters. **Methods:** Alternate comb-like slots are placed on the microstrip patch and the slot dimensions are varied to observe the effect on the antenna performance parameters. The design is simulated in the Mentor Graphics software package. The Mentor Graphics software results are verified with Finite Difference Time Domain (FDTD) analysis in MATLAB. The measured results on the Vector Network Analyzer (VNA) are in good agreement with the simulated results. **Findings:** A dual-band operation resonating at 2.25 GHz and 3.5 GHz is observed. The return loss of -30.23 dB and -33.3 dB at 2.25 GHz and 3.5 GHz is noticed. The gain and directivity at 2.25 GHz are 4.11 dBi and 6.2 dBi; whereas, at 3.5 GHz it is 4 dBi and 6.8 dBi respectively. It is observed that the slot width significantly influences the impedance matching. The alternate arrangement of comb-like slots on the patch increases the electrical length and improves the Return Loss (S11). **Novelty:** Enhancement of S11 characteristics without significant shift in the resonating frequency by felicitous placements of comb-like slots is the novelty of the proposed work.

Keywords: Slotted Antenna; Dual Band; FDTD; UPML; Return Loss (S11)

1 Introduction

As the number of Internet of Thing (IoT) devices are increasing day by day, the design of multifrequency miniaturized antennas is the foremost consideration by the researchers. According to CISCO IBSG about 50 billion devices are connected with the Internet of Things (IoT)⁽¹⁾. The slot dimensions influence the modes in which the antenna operates, an Integrated Waveguide (SIW) based triangular ring slots and its effect on the individual resonant frequency is discussed in⁽²⁾. The frequency ratio and isolation between the bands in case of multifrequency antenna is presented in⁽³⁾. In the work⁽⁴⁾ an asymmetric feed to create additional modes and its flexibility to tune the slotted

structure resulted in required frequency ratio with increased gain is demonstrated. Slotted structures have been widely used to attain wideband performances^(5,6). Meta surface and fractal antennas offer miniaturization with improved performance^(7,8). The antenna performance parameters have been compromised in achieving multiband operation with E-shaped sectorial microstrip antenna is discussed in⁽⁹⁾. Different methods of antenna fabrication have been investigated recently; an embroidery-based fabricated bow-tie antenna is investigated in⁽¹⁰⁾. Polarization diversity is also the main parameter often experimented with slot antennas. Annular slots and appropriate placement with inductor and capacitor between them provide choice to tune the structure to a required sense of polarization⁽¹¹⁾. A dual-polarization has been obtained with the help of a horizontal stub, L-shaped strip with slotted ground plane⁽¹²⁾. Multiple Input Multiple Output (MIMO) antenna for increasing the channel capacity is presented in⁽¹³⁾. Different slotted structures at the different positions on the patch antenna offer multifrequency as well as wideband performance. A meandered cross-shaped slot yields better performance in ultra-high Radio Frequency Identification (RFID) applications⁽¹⁴⁾. In future wireless communication, millimeter and microwave applications need to work with a single system where the high-frequency ratio between the higher and lower frequency is needed. Two separate antennas are designed to achieve the required frequency ratio⁽¹⁵⁾. A dual-band antenna design using Artificial Neural Network (ANN) is reported in⁽¹⁶⁾. Diagonally truncated corners and a Split Ring Resonator (SRR) give polarization flexibility⁽¹⁷⁾.⁽¹⁸⁾ FDTD analysis of fractal antenna for satellite communication is presented. FDTD is an efficient tool in the electromagnetic analysis with real-time visualization of radiating fields^(19,20). A combination of slots with fractals helps to improve bandwidth as well as gain with light compromise in the quality factor of the antenna⁽²¹⁾. A one-dimensional and two-dimensional leaky-wave antenna to detect cancer cells is presented in⁽²¹⁾.

The present work elucidates a complimentary comb-like slotted antenna. The proposed antenna provides dual frequency operation. The parametric variation in slot length and width gives a perceptible improvement in the antenna characteristics. A decrease in the slot width gives improved return loss and radiation characteristics. The slots enhance the radiation capability of the antenna by increasing its electrical length. Parametric optimization gives more enhanced performance. The antenna performance with and without slots is compared. It is observed that, the antenna gives a noticeable improvement in the return loss characteristics with trivial shift in the frequency bands. Both the bands are isolated and operate independently at 2.25 and 3.5 GHz. A frequency ratio between the higher and lower band is found to be 1.55. A FDTD analysis is performed on proposed antennas with wide slots and miniaturized slots to observe the electromagnetic behavior of the antenna. The results from IE3D and FDTD simulations closely match.

2 Methodology

Initially, a simple rectangular patch antenna is designed for Wireless Local Area Network (WLAN) by considering the empirical equations. The antenna is edge-fed and optimized to achieve a dual-band performance. Table 1 and Table 2 shows the specifications and dimensions of the antenna. The slots of width 3 mm and length 14 mm have been placed on the microstrip patch. The slot width and length are optimized to obstruct the path of current flow and to improve the return loss characteristics. Figure 1 depicts the images of antenna. The proposed antenna was simulated in ZELAND IE3D software. Figure 1 shows the development of the geometry from initial rectangular patch to the final optimized geometry.

As a parametric study, the length, width and position of the slots are varied to obstruct the path of current distribution. The feed dimensions and position are optimized for impedance matching at the feed location. Figure 2 shows Antenna 3 and the surface current distribution. Slots of 1 mm wide and 18 mm long are symmetrically and alternatively placed on the microstrip patch in Antenna 3.

Table 1. Design specifications

Design Variables	Values
Frequency Dielectric constant Height of the substrate	2.4 GHz 4.4 1.56 mm

Table 2. Designed dimensions

Design Variables	Values in mm
Length of the ground Width of the ground Length of the Patch Width of the Patch	40 50 28 40

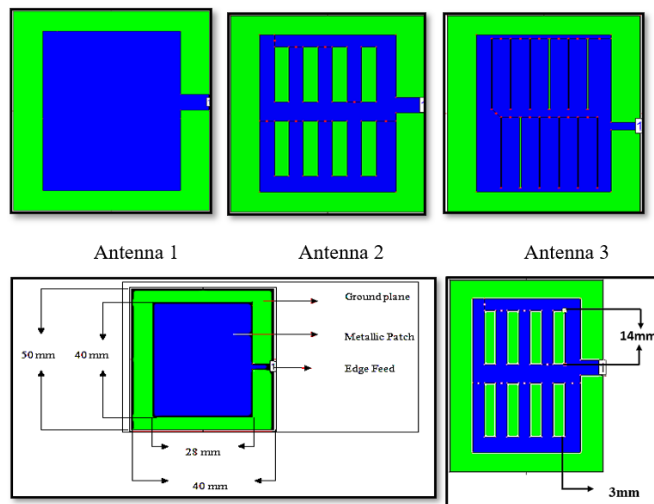


Fig 1. Proposed antennas

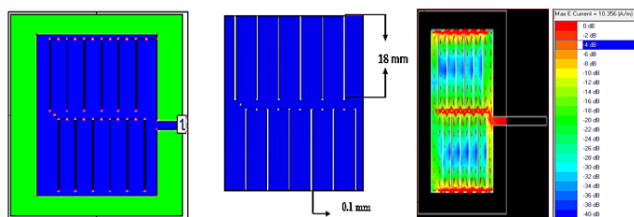


Fig 2. Antenna 3 and current distribution

3 Results and Discussion

Figure 3 shows the overlapped plots of Antenna 1, Antenna 2 and Antenna 3. Figure 3 (a) depicts the information about S11, VSWR in Figure 3 (b), Gain in Figure 3 (c), the directivity in Figure 3 (d). Figure 3 (e) gives information about the axial ratio and polarization.

3.1 Antenna 1

A dual-band performance is observed in Antenna 1, the Antenna 1 is resonating at 2.30 GHz and 3.64 GHz with the S11 value of -22 dB and -17.5 dB. A VSWR value at both the bands is 1.2 which indicates the good matching at the feed. The gain of Antenna 1 at the first band is 3.2 dBi and at the second band is 4.2 dBi. The directivity value is 3.4 dBi and 4.4 dBi, respectively. -10 dB bandwidth at both the bands is 18.75% and 11.20% respectively. The frequency ratio of the higher band to the lower band is 1.5826. The antenna is circularly polarized at both the bands with an axial ratio of 0.7 and 0.3 at lower and higher band, respectively. Figure 3 shows the plots of various parameters of Antenna.

3.2 Antenna 2

As a result of slot insertion, the return loss plot of Antenna 2 at the first band remained unchanged whereas, at the second band, it is enhanced from -17.5 dB to -25 dB. After the insertion of comb-like slots, a slight shift in the frequency bands is observed. A slight shift in the frequency bands is due to the change in surface current distribution. The value of VSWR at both the bands is closely to 1. The gain is slightly improved, at the first band from 3.2 to 3.3 dBi and at the second band from 4.2 to 4.3 dBi. Directivity at the first band is unchanged while at the second band, it is improved from 4.4 dBi to 4.5 dBi. The -10 dB bandwidth is improved in both the bands, in the first band the value is 19.8% and in the second band, it is improved to 15%. The frequency ratio is 1.58. The axial ratio at the first band is 0.7 and at the second band 0.5 which shows that Antenna 2 has retained its circular polarization characteristics in both the bands.

3.3 Antenna 3

As a result of a change in the slot dimensions and placement, the frequency bands are slightly shifted to the left. The band-1 shifted at 2.2 GHz and the band 2 is shifted to 3.5 GHz. The current distribution at the edges of the slots in Antenna 3 is increased as shown in Figure 2, as a result the S11 parameter is enhanced in both the bands at 2.2 GHz with S11 value of -32 dB and at 3.5 GHz with S11 value of -35.2 dB. The gain and directivity are improved, the gain of 3.9 dBi and 4.3 dBi respectively in both the bands is observed. The values of directivity in both the bands are 4 dBi and 4.6 dBi respectively. The improvements are seen at the expense of -10 dB bandwidth. The bandwidth at 2.2 GHz is 16.8% and at 3.5 GHz it is decreased to 8.6%. The frequency ratio of 1.6 is realized. The axial ratio plot shows the value below 1 at the desired frequencies, making it suitable for applications where circular polarization is desired. Figure 3 shows the improvement in the S11 plot from Antenna-1 to the Antenna-3. The antenna with a 1mm wide slot (Antenna-3) shows the better performance compare to the other two. The slight shift in the frequency band is within the tolerance. Table 3 shows the detailed comparison of all three antennas. Improvement in the gain, directivity, return loss and the axial ratio is noticeable. The frequency ratio is within the acceptable range.

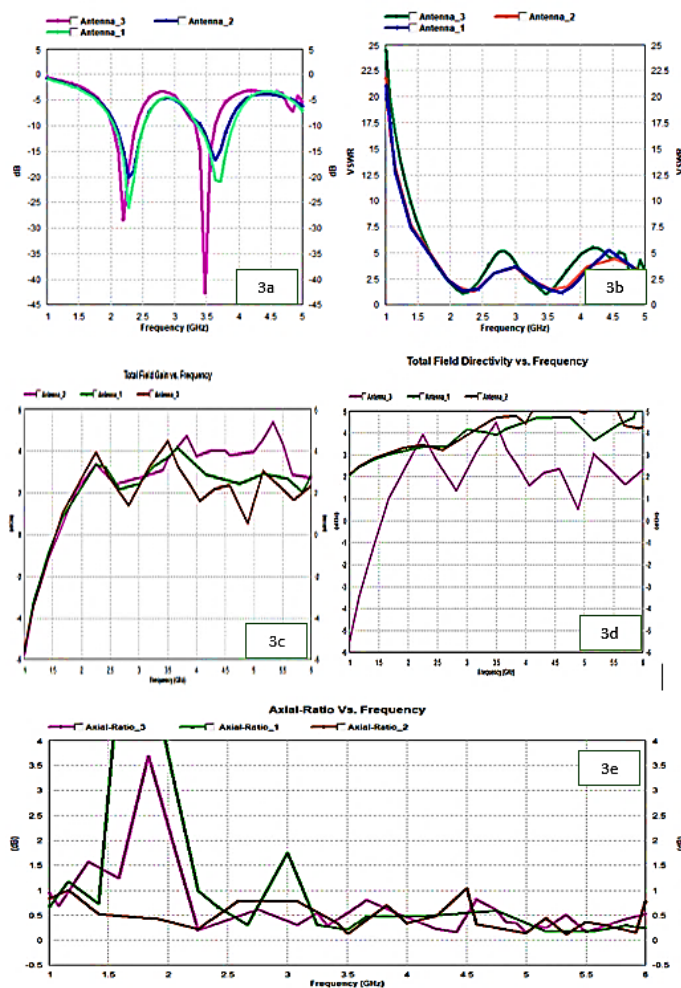


Fig 3. The plots of various parameters of Antenna 1

3.4 Antenna Analysis using FDTD

An FDTD analysis is carried out on Antenna-2 and Antenna-3 to observe the electromagnetic behavior using the concepts explained in [20],[21]. Starting from Maxwell’s curl equations, the update equations are derived using central difference approximation. UPML boundary conditions are used to ensure reflectionless boundaries. The code is simulated in MATLAB.

A Gaussian pulse is used as an input. Yee cell dimensions are chosen to accommodate the smallest dimensions of the geometry. The number of cells in the X directions is chosen as 40 with a cell resolution of 1 mm. 50 cells are taken in Y direction with a cell resolution of 1mm. similarly, 8 cells are taken in the Z direction with a 1mm cell size. Total 4000 iterations are carried out. The images from FDTD simulations of Antenna-2 and Antenna-3 are shown in Figure 6 and Figure 5. The S11 parameters from FDTD simulations resonate at almost the same frequencies as that of ZELAND IE3D simulations as shown in Figure 4.

Table 3. Performance comparison Antenna 1, Antenna 2 and Antenna 3

Parameters	F_r (GHz)	S11	Gain (dBi)	Directivity (dBi)	-10 dB BW	Freq Ratio	Axial Ratio
Antenna 1	2.30 3.64	-22 -17.5	3.2 4.2	3.4 4.4	18.75% 11.20%	1.5826	0.7 0.3
Antenna 2	2.32 3.68	-22 -25	3.3 4.3	3.4 4.5	19.8% 15%	1.58	0.7 0.5
Antenna 3	2.2 3.5	-32 -35.2	3.9 4.3	4.0 4.6	16.8% 8.6%	1.6	4.0 0.1

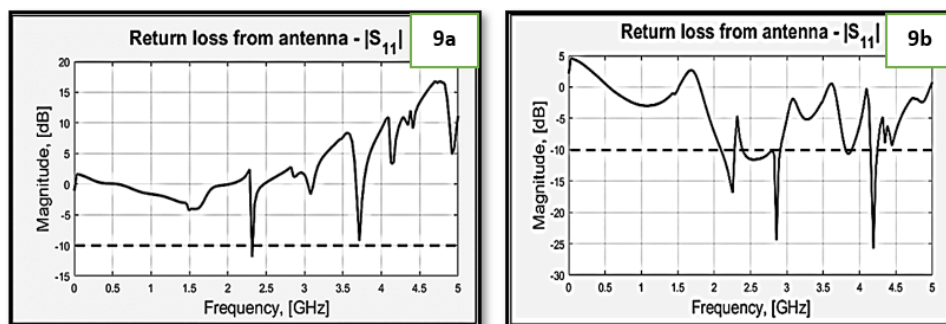


Fig 4. DTD simulated S11 of (a)Antenna-2 and (b) Antenna-3

Table 4. Comparison with existing literatures

Ref.	Frequency Range (GHz)	Dimensions (mm)	Gain (dBi)	Freq Ratio	AR BW
(1)	2.18-2.69, 2.85-3.38	15×33×0.8	---	2	2.17
(2)	14.43-16.49	15.4×32.60×1.57	---	1.142	---
(5)	3.75-10.23, 11.12-12.75	20×20×1	3.678,6.36	---	74.62,12
(10)	2.1-2.9,2.3-2.5	65×55×1.6	2.9-3.4, 4.2-4.7*	1.63,2.41	8.1,4.9,4.3,4.6
(11)	1.45-1.72,1.86-2.29	70×70×1.6	2.5-4	1.286	9,11
(13)	0.902-0.924,0.900-0.923,0.915-0.920	62 × 62 × 1.6	2dBic		7
(14)	5.74-5.9,5.76-5.94	100×100×0.2	10.4/8.5/4.5/9.3 7.3	5.2	---
(15)	3.5 60(fc)	45	2.2dBic	17	
(16)	5.725-5.875	80 × 86 × 2.6 70 × 70 × 1.3	7.3,8.5	---	23
(17)	3.1-4.7	70 × 70 × 1.6		---	3.1,4.2
Proposed (Antenna 3)	2.0-2.38, 3.35-3.65	40× 50 × 1.56	3.9, 4.3	1.6	22.7 14.2

3.5 Measured Results from Vector Network Analyzer

Antenna 2 is fabricated and tested with the help of a VNA. The fabricated antenna is shown in Figure 7. The measured S11 results nearly matches with the simulated results as shown in Figure 8 (a). The slight shift in the bands is due to the production errors, material tolerance and connector losses during the fabrication. VSWR plot in Figure 8 (b) resembles simulated results. The measured results validate the software simulated results. The proposed antenna is suitable for localization and tracking applications. The proposed method of inserting alternate comb-like slots of optimized dimensions is useful in comparison to the existing literature. As this method provides an improvement in the antenna performance without significant shifting in the bands. In future work, the comb-shaped slots can also be experimented with the different feed locations and feeding techniques to arrive at the optimum results without shifting in the frequency bands. In the present work, the method has experimented with line feed for simplicity. Identifying a specific placement of slots can greatly simplify the research in multifrequency antennas which is the focus of this work.

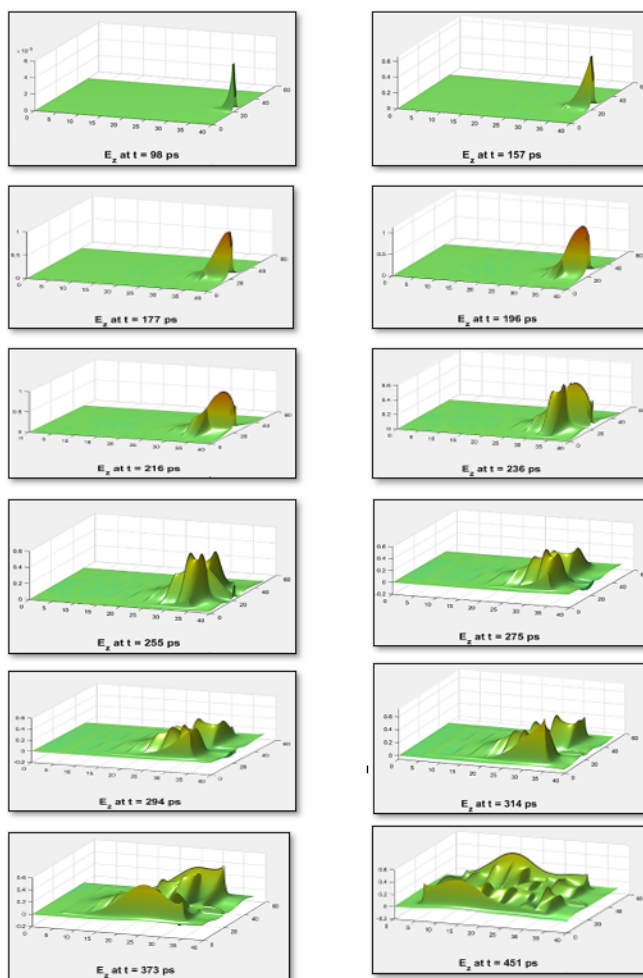


Fig 5. E Field strength of Antenna 3

3.6 Limitations and Future Scope

As the slit width is reduced the fabrication of the proposed antenna becomes impractical, the method may not work in the case of all the shapes of microstrip antennas. As a future scope, the appropriate combination of slits for a particular shape of the antenna can experiment with. The modal study may give more clarity on how the slots influence the modal currents to give a required performance of the microstrip antenna.

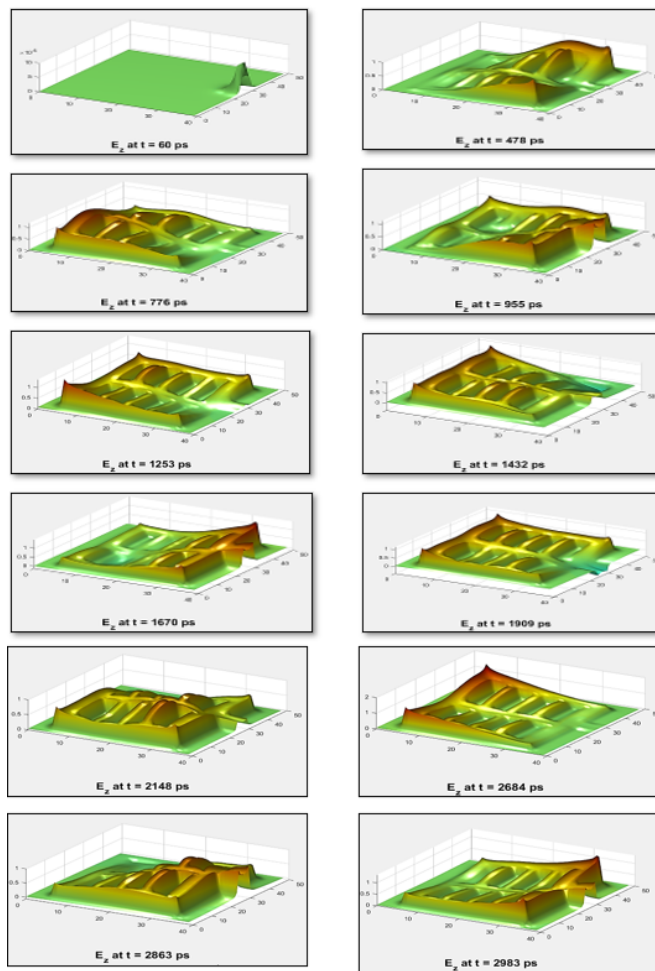


Fig 6. E Field strength of Antenna 2

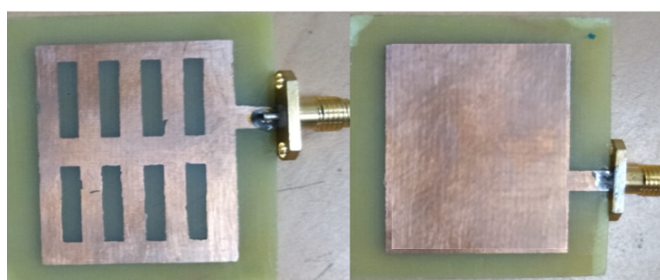


Fig 7. Fabricated Antenna 2

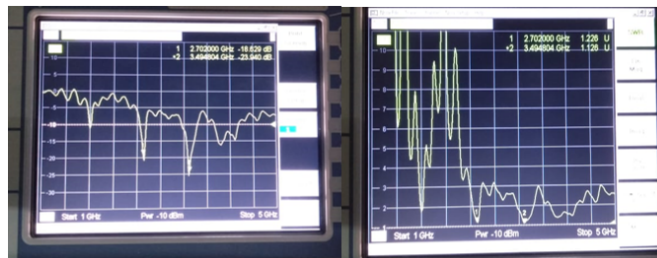


Fig 8. (a) Measured S11 (b) Measured VSWR

4 Conclusion

The proposed antenna shows the improvement in S11 from -22 to -32 and -17.5 to -35.2, Gain is improved from 3.2 dBi to 3.9 dBi and 4.2 dBi to 4.3 dBi, Directivity is improved from 3.4 dBi to 4.0dBi and 4.4 dBi to 4.6 dBi without a significant shift in the resonating frequency with a frequency ratio up to 1.6. A frequency shift of less than 100 MHz is observed. The antenna is circularly polarized thus, making the antenna suitable for location tracking and IoT applications operating at the 2.2 GHz and 3.5 GHz. FDTD analysis and measured results ensures the correctness of the implementation.

References

- 1) Gupta AK, Chowdary PSR, Krishna MV. Trends in IoT Antenna Design-A Brief Review. *Test Engineering and Management*. 2020;p. 193–4120.
- 2) Kumar A, Raghavan S. Broadband SIW cavity-backed triangular-ring-slotted antenna for K-band applications. *AEU - International Journal of Electronics and Communications*. 2018;87:60–64. Available from: <https://dx.doi.org/10.1016/j.aeue.2018.02.016>.
- 3) Chaurasia P, Kanaujia BK, Dwari S, Khandelwal MK. Design and analysis of seven-bands-slot-antenna with small frequency ratio for different wireless applications. *AEU - International Journal of Electronics and Communications*. 2019;99:100–109. Available from: <https://dx.doi.org/10.1016/j.aeue.2018.11.036>.
- 4) Ou JH, Andrenko AS, Li Y, Zhang Q, Tan HZ. High-Efficiency and Wide Frequency Ratio Dual-Band Slot Patch Antenna Utilizing the Perturbed TM₀₂Modes. In: and others, editor. *IEEE Antennas and Wireless Propagation Letters*. doi:10.1109/LAWP.2018.2803775.
- 5) Jaiverdhan, Kumar A, Sharma MM, Yadav RP. Dual wideband circular polarized CPW-fed strip and slots loaded compact square slot antenna for wireless and satellite applications. *AEU - International Journal of Electronics and Communications*. 2019;108:181–188. Available from: <https://dx.doi.org/10.1016/j.aeue.2019.06.027>.
- 6) Varkiani SMH, Afsahi M. Compact and ultra-wideband CPW-fed square slot antenna for wearable applications. *AEU - International Journal of Electronics and Communications*. 2019;106:108–115. Available from: <https://dx.doi.org/10.1016/j.aeue.2019.04.024>.
- 7) Kaur N, Sivia JS, Rajni. Artificial neural network based metasurface inspired planar frequency reconfigurable antenna for wireless applications. *International Journal of RF and Microwave Computer-Aided Engineering*. 2021;31(9). Available from: <https://dx.doi.org/10.1002/mmce.22793>. doi:10.1002/mmce.22793.
- 8) Kalkhambkar G, Khanai R, Chindhi P. Fractals: A Novel Method in the Miniaturization of a Patch Antenna with Bandwidth Improvement, Information and Communication Technology for Intelligent Systems, Smart Innovation. 106 T, Satapathy SC, Joshi A, editors. 2019. Available from: https://doi.org/10.1007/978-981-13-1742-2_63.
- 9) Deshmukh AA, Bagariaparekh T, Mahale S. Mahale Multi-Band Slot Cut E-Shaped Sectoral microstrip Antennas. *Procedia Computer Science*. 2015;49:319–326. doi:10.1016/j.procs.2015.04.259.
- 10) Kapetanakis TN, Pavec M, Ioannidou MP, Nikolopoulos CD, Baklezos AT, Soukup R, et al. Embroidered Bow-Tie Wearable Antenna for the 868 and 915 MHz ISM Bands. *Electronics*. 1983;10. Available from: <https://doi.org/10.3390/electronics10161983jianxing>.
- 11) Patil S, Pandey AK, Pandey VK. A Compact, Wideband, Dual Polarized CPW-Fed Asymmetric Slot Antenna for Wireless Systems. *Journal of Microwaves, Optoelectronics and Electromagnetic Applications*. 2020;19(3):343–355. Available from: <https://dx.doi.org/10.1590/2179-10742020v19i3827>.
- 12) Bhaskar S, Singh AK. Meandered cross-shaped slot circularly polarised antenna for handheld UHF RFID reader. *AEU - International Journal of Electronics and Communications*. 2019;100:106–113. Available from: <https://dx.doi.org/10.1016/j.aeue.2018.12.024>.
- 13) Aliakbari H, Nie LY, Lau BK. Large Screen Enabled Tri-Port MIMO Handset Antenna for Low LTE Bands. *IEEE Open Journal of Antennas and Propagation*. 2021;2:911–920. Available from: <https://dx.doi.org/10.1109/ojap.2021.3107436>.
- 14) Zhang JF, Cheng YJ, Ding YR, Bai CX. A Dual-Band Shared-Aperture Antenna With Large Frequency Ratio, High Aperture Reuse Efficiency, and High Channel Isolation. *IEEE Transactions on Antennas and Propagation*. 2019;67(2):853–860. Available from: <https://dx.doi.org/10.1109/tap.2018.2882697>.
- 15) Nakmouche MF, Allam AMMA, Fawzy DE, Lin DB, Sree MFA. Development of H-Slotted DGS Based Dual Band Antenna Using ANN for 5G Applications. *2021 15th European Conference on Antennas and Propagation (EuCAP)*. 2021. doi:10.23919/EuCAP51087.2021.9411213.
- 16) Kandasamy K, Majumder B, Mukherjee J, Ray KP. Dual-Band Circularly Polarized Split Ring Resonators Loaded Square Slot Antenna. *IEEE Transactions on Antennas and Propagation*. 2016;64(8):3640–3645. Available from: <https://dx.doi.org/10.1109/tap.2016.2565729>.
- 17) Sofi AA, Amit S, Sujatha BK. 3D-FDTD analysis of fractal antenna using PML boundary conditions. *Global Transitions Proceedings*. 2021;2(2):323–329. Available from: <https://dx.doi.org/10.1016/j.gltp.2021.08.029>.
- 18) Tong MS, Sauleau R, Krozer V, Lu Y. Numerical studies of stripline-typed photonic band-gap (PBG) structures using finite difference time domain (FDTD) method. *Journal of Computational Electronics*. 2006;5(1):53–61. Available from: <https://dx.doi.org/10.1007/s10825-006-7984-5>.
- 19) Asif R, Aziz A, Amjad M, Akhtar M, Baqir A, Abbasi MN. Analysis and Design of an Efficient and Novel MIMO Antenna for 5G Smart Phones Using FDTD and FEM. *Applied Computational Electromagnetics Society*. 2021;36(3):266–272. Available from: <https://dx.doi.org/10.47037/2020.aces.j.360306>.

- 20) Bhattacharya A, Roy B, Chowdhury SK, Bhattacharjee AK. Computational and experimental analysis of a low-profile, isolation-enhanced, band-notch UWB-MIMO antenna. *Journal of Computational Electronics*. 2019;18(2):680–688. Available from: <https://dx.doi.org/10.1007/s10825-019-01309-3>.
- 21) Sarabi M. The Application of Leaky Wave Antennas for Medical Hyperthermia Treatment and Beamformer in FMCW Automotive Radar Systems. 2021. Available from: <https://doi.org/10.37099/mtu.dc.etr/1266>.